$$EVM\,(\%) = \sqrt{\frac{P_{error}}{P_{reference}}} \cdot 100\% \tag{4}$$

where $P_{error}$ is the RMS power of the error vector and $P_{reference}$ is the RMS power of the ideal transmitted signal. Here the maximum IEEE 802.11 allowed EVM values of 12.5% for QPSK, 11.2% for 16-QAM and 5.6% for 64-QAM data are assumed as standard criteria for signal quality evaluation.

Figure 3 plots the RMS EVM values, averaged over time, measured for 10, 20 and 40 Mb/s QPSK, 20, 40 and 80 Mb/s 16-QAM while 30, 60 and 120 Mb/s 64-QAM encoding formats versus the subcarrier radiofrequency. In general, as predicted by the phase-to-intensity conversion curve illustrated in Fig. 1(b), the EVM increases at lower frequencies. In case of QPSK we can appreciate that a good signal quality is obtained for the whole frequency range as the EVM is always well below the standard 12.5%, with values below 5% for 20 Mb/s. For 16-QAM and 64-QAM modulations, the highest values, respectively around 14% and 8%, were achieved at one of the lowest frequencies (3 GHz) where, in fact, the major fluctuations of the MMF link response are encountered. In these cases, the channel frequencies comprised between 12 and 20 GHz show, especially at high bit rates, the best signal quality as expected from the high-pass filtering characteristic of the dispersive fiber link.

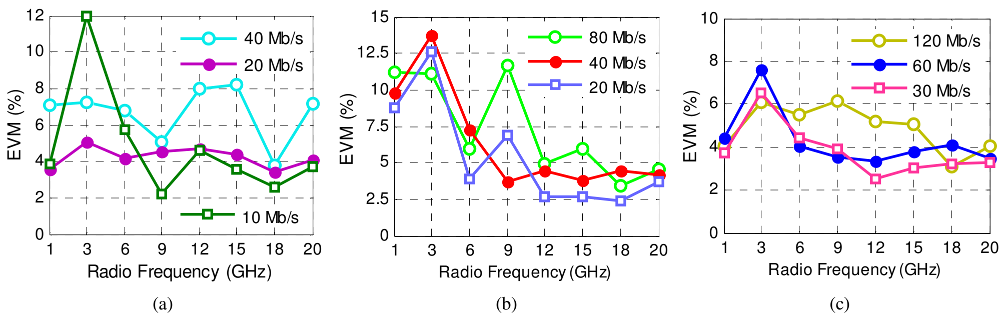


Fig. 3. Measured EVM (%) versus electrical subcarrier frequency for (a) QPSK, (b) 16-QAM and (c) 64-QAM modulation.

The measured constellation diagrams for the determined high-frequency subcarrier region are depicted in Fig. 4 for the three modulation formats under consideration when selecting the higher achieved bit rate for every format, which actually corresponds to a symbol rate of 20 Ms/s. In that case, both the 16-QAM and 64-QAM symbols mostly concentrated well around the reference constellation, while for QPSK a slightly more scattered pattern was obtained, in line with the EVM evaluation shown in Fig. 3. Note that a considerable better location of the QPSK constellation points was reached when decreasing the bit rate down to 20 Mb/s or 10 Mb/s, again in full agreement with the measured EVM. Even so, a good location of the constellation points was achieved in every high-frequency subcarrier for the maximum bit rate transmission. This result relates, in the worst-case scenario, to a minimum signal-to-noise ratio (SNR) of 21.9 dB (maximum EVM of 8%) for QPSK, while 24.6 dB (maximum EVM of 5.9%) for 16-QAM and 25.8 dB (maximum EVM of 5.1%) for 64-QAM, since SNR $\approx 1 / (EVM^2)$ [19]. The bit error rate (BER) can be actually related to the measured RMS EVM by applying the following equation for a general $M$-ary modulation system [19],

$$P_b \approx \frac{2(1-1/L)}{\log_2 L} Q\left[\sqrt{\left(\frac{3\log_2 L}{L^2-1}\right)\frac{2}{EVM^2 \log_2 M}}\right], \tag{5}$$

#162081 - $15.00 USD Received 30 Jan 2012; revised 12 Apr 2012; accepted 18 Apr 2012; published 9 May 2012

where $L$ represents the number of levels in each dimension of the $M$-ary modulation format and $Q$ is the Gaussian co-error function. The evaluation of Eq. (5) allows us to corroborate that error-free transmission has been successfully demonstrated since the measured EVM figures are translated into computed BER values well below $10^{-15}$ and $10^{-12}$ respectively for QPSK and 16-QAM modulations, while around $10^{-6}$ for 64-QAM, which, if required, could be improved by properly applying error correction coding.

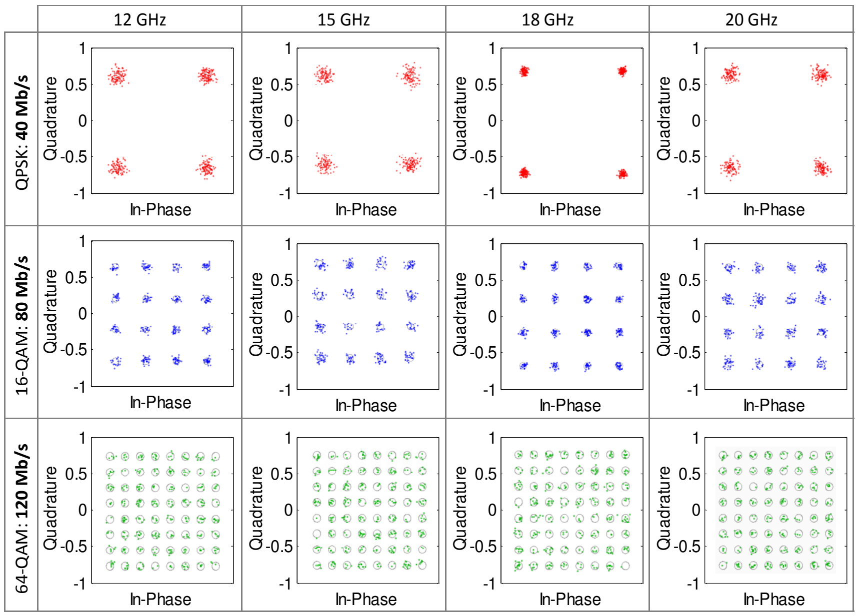


Fig. 4. Measured constellation diagrams for different modulation formats and bit rates at the subcarrier channel frequencies ranging from 12 to 20 GHz.

## 3. Practical considerations

Although the reported results were computed for the case of independent single subcarrier transmission they nevertheless show the possibility of further increasing the total capacity if more channels are accommodated in the operative microwave region determined by the phase-to-intensity conversion process. Figure 5 depicts a schematic of the proposed multichannel SCM signal distribution. The modification of the evaluated experimental setup in order to consider simultaneous transmission, i.e. real implementation of subcarrier multiplexing (SCM), would require taking into account the harmonic and intermodulation distortion arisen in the system. An estimate of the impact of these sources of impairment has been provided in a previous work by the authors [22,23], where the evaluation of the impact of second and third order distortions through the analysis of the Composite Second Order (CSO) and the Composite Triple Beat (CTB) parameters showed the potential feasibility of implementing subcarrier modulation techniques in MMF links. In particular and referring to the case depicted in Fig. 5, the possible nonlinearities due to the RF multiplexing stage and subsequent modulation circuitry should be limited or compensated to avoid them from becoming a dominant source of impairment. Under those conditions, the theoretical analysis carried out in [22] showed that for an application case as the one reported in this paper, (typical modulation index value of $m = 0.01$ as well as usual fiber parameters), the distortion will have a negligible impact in ROF transmission with high requirements (CSO < –50 dBc).

#162081 - $15.00 USD Received 30 Jan 2012; revised 12 Apr 2012; accepted 18 Apr 2012; published 9 May 2012

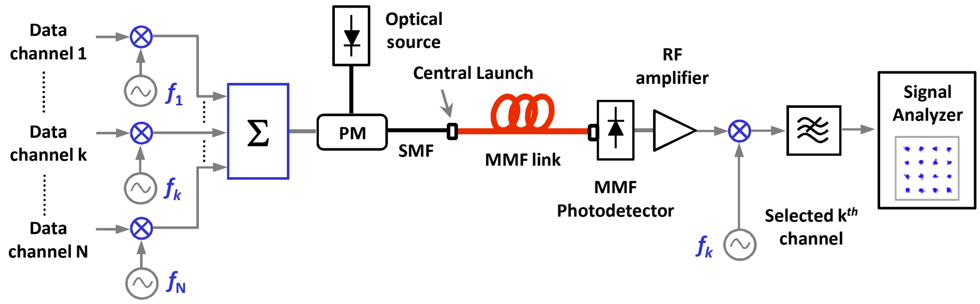


Fig. 5. Multichannel SCM signal distribution in the proposed phase-modulated MMF link.

Also, as it has been previously mentioned, a more complete analysis including the impact of modal noise on the system nonlinearities could be carried by adapting the model developed in [20] to the specific case of external phase modulation. Under achievable practical conditions, that is using good quality connectors and central launching technique, the impact of modal noise on the system's performance, including nonlinearities, is expected to be low [19]. Under these conditions, the experimental results reported in [23] for the transmission of high-frequency subcarrier multiplexed CATV channels under linear intensity modulation can provide a good indication, as PM is inherently linear. These results showed that the CSO and CTB penalty due to MMF transmission yield values in the range of 3 to 7 dB.

By optimizing both the modulator and the detector responses for frequencies up to 30 GHz and reducing the channel spacing down to 100 MHz, a total of 240 data channels can be allocated in the operative spectrum region comprised between 6 and 30 GHz. In consequence, and assuming a linear capacity x distance product typical of few mode MMF links, a potential aggregate bit rate per length product of 144 Gb/s·km could be achieved for the 5 km MMF link under evaluation. For that purpose, nonlinearities due to potential saturation of the detector arising from high peak-to-average power ratio would need to be bounded. A feasible technique could be that which is currently implemented to avoid clipping in direct-modulation laser based CATV systems by independently randomizing the initial phase of each subcarrier channel.

## 4. Conclusions

A broadband phase-modulated MMF link has been successfully demonstrated for the first time to our knowledge by subcarrier transmission of high-frequency digital passband channels for bit rates up to 120 Mb/s. A cost-effective solution is presented in which a simple demodulation process is accomplished taking advantage of the phase-to-intensity conversion characteristic of a 5-km-length dispersive fiber link. The combination of the central launching technique and the use of low linewidth lasers contributed to the demonstrated capability of ROF transmission well beyond the typical MMF bandwidth-distance.

A satisfactory EVM was measured for subcarrier channels placed above 6 GHz for QPSK, 16-QAM and 64-QAM modulation formats. The total transmission capacity of the proposed phase-modulated MMF link can be enhanced by accommodating more passband channels in the phase-to-intensity-conversion operative frequency range and by combining the proposed subcarrier multiplexed approach with wavelength division multiplexing techniques.

## Acknowledgments

The authors wish to acknowledge the financial support given by the Research Excellency Award Program GVA PROMETEO 2008/092.